Pergamon

Bioorganic & Medicinal Chemistry Letters 12 (2002) 2899–2905

BIOORGANIC & MEDICINAL CHEMISTRY LETTERS

# Molecular Modeling and Enzymatic Studies of the Interaction of a Choline Analogue and Acetylcholinesterase

Stefano Alcaro,[a,*] Luigi Scipione,[b] Francesco Ortuso,[a] Salvatore Posca,[b] Vincenzo Rispoli[a] and Domenicantonio Rotiroti[a]

[a]*Dipartimento di Scienze Farmacobiologiche, Università degli Studi 'Magna Græcia' di Catanzaro, Complesso 'Ninì Barbieri', I-88021 Roccelletta di Borgia (CZ), Italy*

[b]*Dipartimento di Studi di Chimica e Tecnologia delle Sostanze Biologicamente Attive, Università degli Studi 'La Sapienza' di Roma, P. le A. Moro, 5, 00185 Rome, Italy*

Received 20 December 2001; revised 3 May 2002; accepted 12 July 2002

**Abstract**—Pivaloyl-choline iodide **1** interactions with acetylcholinesterase (AChE) have been studied by theoretical and enzymatic methods. An integrated computational approach has clearly shown a substrate rather than inhibitory profile for **1**. Enzymatic experiments have also supported the same theoretical conclusion indicating that AChE was able to hydrolyze **1** to choline.


Alzheimer's disease (AD) is a common neuro-degenerative disorder characterized by the deterioration of the basal forebrain cholinergic neurons, which results in marked deficits in the neurotransmitter acetylcholine (ACh).[1] The actual therapy is based on the use of drugs inhibiting the acetylcholinesterase (AChE), that catalyzes the hydrolysis of the ACh within the intersynaptic area thus increasing its concentration.[2] Currently approved drugs do not lack in toxicity and side effects.[3] Therefore, the research for pharmacological alternatives is still very active. This study takes into account compound **1** (Fig. 1), which is structurally related to ACh as a candidate drug able to increase the cerebral level of choline and consequently enhance the biosynthesis of acetylcholine.

The chemical similarity to the neurotransmitter makes this molecule a possible candidate ligand for any macromolecule interacting with the ACh such as, cholinergic receptors and the reuptake system of the cholinerigic synapses or AChE.

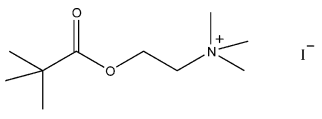


**Figure 1.** Structure of **1**.

In fact, owing to the lipophilic character of the pivaloyl moiety, **1** should be able to cross the blood–brain barrier (BBB) and release choline into the brain as well as reported for other neurotransmitters.[4]

In this study, the ability of compound **1** to interact with the AChE and undergo hydrolysis to choline has been taken into account.

In order to clarify these aspects a theoretical study has been carried out with the aim to evaluate the steric and electronic features of **1** with respect to ACh in the AChE active site. Furthermore, a series of enzymatic tests to ascertain if **1** can be hydrolyzed by the AChE have been conducted.

The molecular modeling work has been carried out with some preliminary operations followed by three different computational steps. Basing on the well known mechanism of interaction between the neurotransmitter and the enzyme, only the cation portion of compound **1** and ACh has been considered.

At the beginning of the work, all the Protein Data Bank (PDB) models reporting the interaction of the AChE with several compounds have been analyzed.[5]

*Corresponding author. Fax: +39-0961-391490; e-mail: alcaro@unicz.it

0960-894X/02/$ - see front matter 
PII: S0960-894X(02)00554-1

One such structure[6] reported the transition state adduct between the enzyme and its natural substrate ACh. This was chosen for the preliminary operations because of the strong similarity with our derivative **1**.

In order to apply an implicit model of solvation to our energy calculations, all the water molecules were removed from the reference model. Then, the amino acid residues within 10 Å from the Ser200 corresponding to the active site of the enzyme were selected. The complete list of the 109 residues matching our selection is reported in Table 4 of the Supplementary Material. The covalent bond between ACh and Ser200 of AChE has been deleted and all the non-aliphatic hydrogen atoms have been added obtaining an AMBER*[7] united atoms model of the AChE active site complexed to the natural substrate (E·ACh). After AMBER* steric energy calculations,[8] the net charge of our model was analyzed to check the consistency with the presence of 12 negative and four positive charged residues including the ACh cation ligand.

After these preliminary operations, the model still maintained the conformation of the enzyme active site as in the original PDB structure. The isolation of the active site of AChE has prompted us to adopt a constrained minimization protocol for the model obtained after the preliminary operations. The idea to adopt such a computational approach is supported by the average root mean square (RMS) deviation computed using the atomic coordinates of the peptide backbone between the active site of the 2ACE model and other seven AChE three-dimensional structures published in the PDB.[9] The small average RMS value of 0.27 Å suggests that we keep fixed the well conserved backbone conformation of AChE in our constrained energy minimization. The following models have been taken into account: the enzyme only (E), the complex E·ACh from the preliminary operation, and the complex AchE·**1** (E·**1**) obtained by replacing the acetyl moiety with the pivaloyl group. According to the standard MacroModel protocol, a force constant of 100 kcal/mol Å$^2$ to the C, O, N, and H atoms of the AChE backbone has been applied. The energy constrained minimizations have been performed using the following protocols: force field AMBER* united atom notation, GB/SA water implicit model of solvation,[10] and 10,000 iterations with the Polack Ribier Conjugate Gradients (PRGC) method until the standard convergence criterion of 0.01 kcal/mol Å has been achieved.

In order to highlight the internal complexation and solvation energy differences between the active site AChE recognition of **1** with respect to the natural substrate ACh, both enzyme and ligand conformations isolated from the energy minimized complexes have been submitted to an energy calculation in the same conditions. Three-dimensional mapping calculations have been accomplished using representative GRID probes.[11] This analysis has been performed using the atomic coordinates of the complexes E·ACh and E·**1** obtained after the constrained energy minimization. The peptide residues of both molecular models have been processed with the appropriate GRID probes and resolution.[12]

Since the first step of the catalytic reaction between the AChE and the natural substrate implies a nucleophilic attack from the Ser200 hydroxyl oxygen to the carbonyl carbon of the acetylcholine, this atom must be characterized by an adequate and consistent positive charge. In order to compare the charge distribution of **1** with respect to the ACh substrate, some molecular mechanics, semi-empirical, and ab initio calculations[13] have been performed especially looking at the results on the quaternary ammonium atom N+ and the ester carbon of both molecules.

The two constrained energy minimizations starting from the geometry obtained from the PDB model 2ACE allowed us to make direct comparison of the recognition processes between the natural substrate and the pivaloyl derivative into the catalytic portion of the AChE active site.

The structural comparison revealed that the interactions between the two ligands and the enzyme are very similar. Two hydrogen bonds between the sp$^2$ oxygen atom and the amide hydrogen atoms of Gly118 and Gly119 stabilize the complexes anchoring the ligands in the same orientations. On the other hand, electrostatics also play an important role because both ligands contain one positive net charge and there are several oppositely charged aminoacid residues in the active site. The position with respect to the anionic site within the gorge is evaluated as the distance between the dummy atom centered in the aromatic six-membered ring of the TRP 84 side-chain and the quaternary ammonium. In both ligands this distance is conserved after the constrained energy minimization; 4.165 and 4.175 Å in the E·ACh and E·**1** complexes, respectively. The distance between the hydroxyl oxygen atom of the Ser200 and the sp$^2$ ester carbon of the ligands represents another interesting geometrical description because it is responsible for the catalytic attack on the substrate.

This distance is quite short; 2.897 and 2.884 Å in the E·ACh and E·**1** complexes, respectively (Fig. 2). After the energy minimization, the active site of the enzyme endures small conformational changes as revealed by the RMS deviation of 0.279 Å in the atomic coordinates between two complex models. The steric effect of the *t*-butyl moiety in the E·**1** complex produces relevant changes on the Phe331 and Phe330 side chain conformation only (Fig. 2). Starting with the energy minimized structures 1000 ps backbone constrained molecular dynamic simulation per complex were carried out along with 100 sampled conformations that were multi minimized with the same force field and solvation conditions. The average distances from Ser200 and the sp$^2$ ester carbon of the ligands were both 3.150 Å. No other energy minimum lower than those originally considered were found during the dynamic simulations.

In order to make a detailed energy analysis of the minimized complexes, the differences in total, GB/SA water solvation and interaction energies have been computed and reported in Table 1.

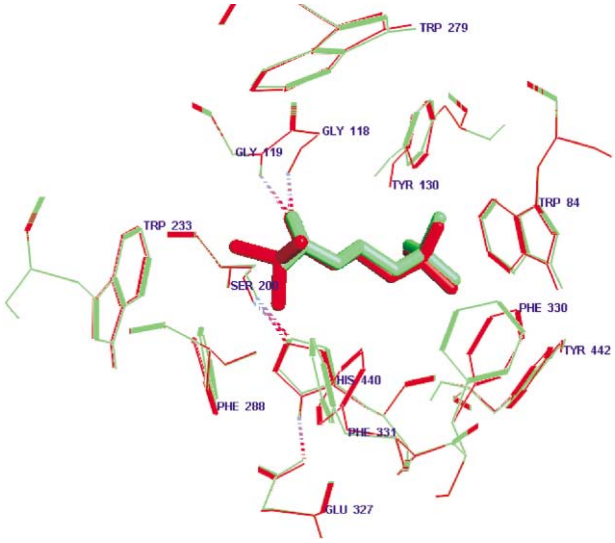


**Figure 2.** Superimposition between the E·Ach (green) and E·**1** (red) complexes after the constrained energy minimization. Two hydrogen bonds Gly118–119 residues anchor the ester Oxygen of the ligands. The quaternary ammonium is clearly surrounded by the aromatic residues Tyr442, Phe330, Tyr130 and Trp84. With this last aminoacid is evident the π–cationic interaction.

**Table 1.** AMBER* energy comparison in kcal/mol after backbone constrained minimization in GB/SA of the E·ACh and E·**1** complexes

| Molecular system | $\Delta_{1\text{-ACh}}$ total E | $\Delta_{1\text{-ACh}}$ GB/SA $H_2O$ solvation E | $\Delta_{1\text{-ACh}}$ intermolecular E |
|---|---|---|---|
| [Enzyme·Ligand] | −3.67 | −10.90 | −3.25 |
| Ligand from [E·L] | | 1.80 | |
| Enzyme from [E·L] | −4.50 | −12.80 | |

The total energy of the E·**1** complex is lower than the E·ACh one even if the different internal energies of each ligand make this comparison not as rigorous. The more correct comparison is between the solvation energies. The $\Delta E\text{solv}_{1\text{-ACh}}$ is more favorable for the E·**1** indicating that in this complex fewer hydrophobic residues are exposed to the solvent. The difference is quite large (10.9 kcal/mol). According to other studies,[14] it has been confirmed that the solvation effect plays a crucial role in the mechanism of AchE–ligand recognition.

The solvation energies of the two ligand conformations extracted from the energy minimized complexes are also in agreement with a higher level of hydrophobicity of **1** that is less favored to be solvated by water than the natural neurotransmitter. In this case, the $\Delta E$ is only 1.8 kcal/mol but can contribute to force the pivaloyl derivative into the active site of the enzyme.

The comparison between the AChE interaction energies is also favorable to the **1** ligand with respect to ACh. In both complexes the absolute intermolecular energies are very attractive (data not shown) mainly due to the formation of two hydrogen bonds and to the electrostatic term (Fig. 2). In this case the energy discrimination of 3.25 kcal/mol is more favorable for [E·**1**] and can also be addressed to the different Van der Waals contributions

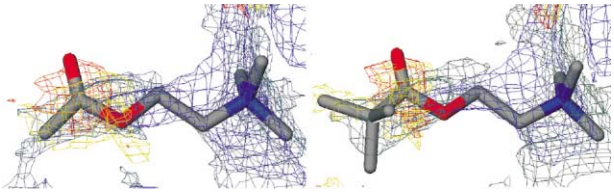

**Figure 3.** Comparison between the GRID density map distribution of complexes E·Ach (right) and E·**1** (left). For clarity the, enzyme structure has been omitted. GRID probes: *O* for the carbonyl oxygen (red map), *OES* for the ester oxygen (orange map), *NM3* for the trimethylammonium moiety (blue map) and *C3* for the methyl and methylene groups (gray map).

of the hydrophobic residues Phe331, Phe288, and Trp233 closest to the *t*-butyl moiety as shown in Figure 2.

The GRID results are displayed in terms of density distribution of four probes as shown in Figure 3. The different GRID probe chemical-physical characteristics have prompted us to adopt different energy thresholds (ET) in the map display generation. The red and the orange maps are related to the carbonyl *O* (ET = −6.5 kcal/mol) and ester *OES* (ET = −3.0 kcal/mol) oxygen probes respectively. In both cases, the location of the closest energy minimum map to each ligand has clearly delimited the area where the oxygen atoms are present in both ACh and compound **1**. Actually, the ester moiety contains both the oxygen probes (*O* and *OES*) whose three-dimensional locations are correctly predicted by the GRID probes.

Also the prediction of the best location for the trimethylammonium moiety has perfectly matched with the coordinates of the quaternary nitrogen as shown by the blue maps corresponding to the NM3 (ET = −8.5 kcal/mol) probe.

More interesting, in our opinion, are the results obtained with the probe shown as gray maps C3 (ET = −3.5 kcal/mol). In both complexes there are two distinct maps where the probe has reached the energy minimum. The first one fits very well with the location of the three methyl groups attached to the quaternary nitrogen. Again this is a good GRID prediction that validates the method. Notably this area extends itself toward the exposed part of the gorge corresponding to the entrance of the active site of the enzyme. Some known AChE inhibitors have shown several carbon atoms located exactly in this first C3 probe area.[15] The second one, surprisingly, corresponds to the ester terminal part of ACh and **1**. This area has included most of the ester moiety and predicted an energetically favored position for derivative compounds based on the introduction of methyl groups onto the acetyl terminal of ACh. Actually, introducing the pivaloyl group, as in compound **1**, the corresponding C3 probe map has included the whole *t*-butyl moiety.

The charge calculation carried out using the molecular mechanics force field AMBER* on the compounds ACh and **1** has revealed no discrimination between the two

most important atoms responsible for the binding and the reactivity of these ligands with AChE. The reason should be explained by the intrinsic approximation of the charge calculation method based only on the bond connectivity. Moreover, the quaternary nitrogen is not evaluated with a partial positive charge even if the three moderately positive charged methyl groups contribute to balance this unexpected result (Table 2). Therefore, more sophisticated and accurate methods have been used. Actually, the semi-empirical AM1 electrofit and the ab initio 3-21 G* electrofit charge distributions have been in agreement to assign a consistent partial positive charge larger than 0.25 to the quaternary ammonium atoms. As far as the $sp^2$ carbon atom is concerned, it is evaluated strongly positive in any case (Table 2). The full list of the charge distribution is reported in Table 5 of the Supplementary Material.

The enzyme–ligand interaction in the E·ACh and E·**1** complexes evaluated by constrained energy minimization with AMBER* and GB/SA water reveal structurally and energetically the same kind of recognition in the formation of the Van der Waals complex, which is the prerequisite of the catalytic reaction. The solvation effect seems to play an important role in the energy stabilization E·**1** complex with respect to the E·ACh one.

The GRID calculations have demonstrated to be very effective in the prediction of the most favored location of the different atom types constituting both ligands. In particular the C3 probe is able to confirm that the introduction of methyl groups in the acetyl terminal moiety of ACh can improve the binding properties.

The two different computational approaches followed in this study are in agreement to establish that compound **1** can be easily incorporated into the active site of AChE and can follow the same recognition process of ACh.

The charge distribution comparison on the crucial $sp^2$ carbon atom involved in the first step of the ester reaction confirms equal probability of ACh and **1** to be attacked and catalyzed by the AChE enzyme.

In order to support these theoretical calculations with experimental data, a series of enzymatic tests able to reveal if **1** may be a substrate of AChE were carried out. First, a kinetic assay of AchE[16] according to the Ellman method[17,18] has been performed to obtain the standard Lineweaver–Burk plot. These set of rate determinations were repeated by adding AChE solutions preincubated for

**Table 2.** Formal charge distribution computed on the quaternary ammonium and the $sp^2$ carbon atoms with MacroModel (AMBER* FF), semi-empirical AM1 and 3–21 G* methods

| Method | Compd | Quaternary ammonium N+ | Ester $sp^2$ carbon |
|---|---|---|---|
| AMBER* | ACh | −0.024 | 0.600 |
| | **1** | −0.024 | 0.600 |
| AM1 Electrofit | ACh | 0.264 | 0.793 |
| | **1** | 0.316 | 0.760 |
| 3–21 G* Electrofit | ACh | 0.245 | 0.909 |
| | **1** | 0.254 | 1.049 |

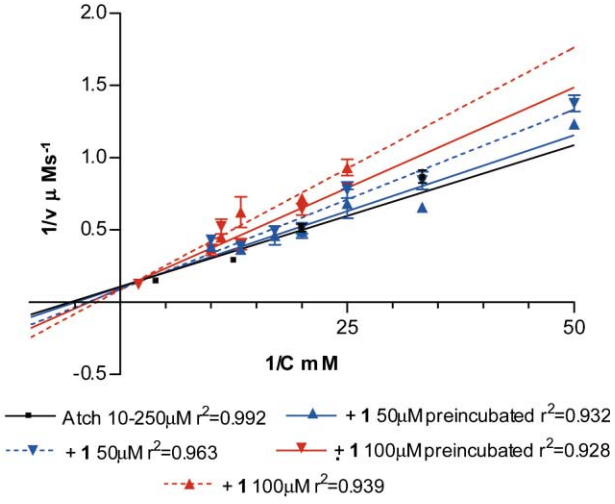


**Figure 4.** Lineweaver–Burk plot obtained with Atch alone (10–250 mM) and in presence of compound **1** 50 mM (blue curves) and 100 mM (purple curves) with preincubation delay (continuous lines) and without preincubation (dashed lines).

**Table 3.** Primary kinetic data obtained using the Ellman's method[a]

| 1/C ($mM^{-1}$) | AtCh 10–250 μM | | + **1** 50 μM | | + **1** 50 μM preincubated | | + **1** 100 μM | | + **1** 100 μM preincubated | |
|---|---|---|---|---|---|---|---|---|---|---|
| | 1/v ($sμM^{-1}$) | SEM | 1/v ($sμM^{-1}$) | SEM | 1/v ($sμM^{-1}$) | SEM | 1/v ($sμM^{-1}$) | SEM | 1/v ($sμM^{-1}$) | SEM |
| 100.0 | 2.033 | 0.081 | | | | | | | | |
| 50.0 | | | 1.377 | 0.097 | 1.231 | 0.006 | | | | |
| 33.3 | 0.869 | 0.043 | 0.841 | 0.105 | 0.658 | 0.010 | | | | |
| 25.0 | | | 0.777 | 0.095 | 0.682 | 0.099 | 0.932 | 0.099 | 0.789 | 0.016 |
| 20.0 | 0.514 | 0.026 | 0.514 | 0.065 | 0.491 | 0.047 | 0.719 | 0.033 | 0.644 | 0.070 |
| 17.0 | | | 0.495 | 0.036 | 0.461 | 0.065 | | | | |
| 13.3 | | | 0.386 | 0.033 | 0.366 | 0.026 | 0.623 | 0.150 | 0.402 | 0.054 |
| 12.5 | 0.297 | 0.021 | | | | | | | | |
| 11.1 | | | | | | | 0.450 | 0.022 | 0.525 | 0.087 |
| 10.0 | | | 0.430 | 0.047 | 0.387 | 0.032 | 0.374 | 0.008 | 0.361 | 0.052 |
| 4.0 | 0.148 | 0.010 | | | | | | | | |
| 2.0 | | | | | | | | | 0.125 | 0.005 |

[a]Compound **1** was used at 50 and 100 μM with and without 30 min of incubation delay. Each kinetic run was triplicate.[18]

30 min with **1** (50 and 100 μM) and the effects on the Lineweaver–Burk plot were evaluated. The same procedure was repeated using the same reactant concentrations without any incubation delay. The analysis of the kinetic data obtained from the preincubated data set show a negligible AChE inhibition effect at lower concentration of **1** (50 μM) that is otherwise evident at the higher concentrations (100 μM) (Fig. 4). Considering the non-preincubated data set these effects of inhibition are much more evident both for 50 and 100 μM of compound **1** with respect to the corresponding preincubated set of data. All the obtained curves were in good agreement with the reported mechanism of competitive inhibition.[19]

The reduced inhibition activity of **1** when preincubated with AChE should be explained with the hydrolysis of this compound by the enzyme, which was probably incomplete at the higher concentration as showed by a residual inhibition activity at 100 μM. Probably, during the time of incubation of the enzyme with compound **1** the hydrolysis of **1** took place rather than the enzyme inhibition, thus suggesting that this compound should be a substrate rather than an inhibitor (Fig. 4).

The primary kinetic data are reported in Table 3.

Moreover a set of $^1$H NMR experiments were carried out with the aim of demonstrating the hydrolysis of **1** by AChE.[20] A $^1$H NMR spectra of compound **1** ($10^{-3}$ M in 0.6 mL of $D_2O$/0.01 M pH 7.4 phosphate buffer 1:1) was recorded and only the signals relative to compound **1** can be detected; this solution was added to 0.4 U of AChE and then stored at 25 °C for 24 h and a new proton spectra was taken to verify the presence of compounds other than **1**.

In the described conditions other than compound **1** a new series of signals can be detected, which can be attributed to the choline and the pivalate ions. The molar ratio found for compound **1** in pivalate and choline, was 3.8, 3.1, and 3.1, respectively, which corresponds to about 55% of the hydrolysis of compound **1**. The nature of the substances was confirmed by comparison with an equimolar mixture of authentic samples of choline iodide and sodium pivalate in the same conditions. This experiment was repeated without AChE and no autohydrolysis of compound **1** was detected (see Fig. 5 of Supplementary Material).

This study clarifies by the combination of theoretical and experimental approaches that the compound **1** is a substrate for the AChE enzyme.

## Acknowledgements

This work was financially supported by '40%' M.U.R.S.T. funding and *Consiglio Nazionale delle Ricerche* funding (grant code CNRC004507_002, Agenzia-2000). The authors thank the *Istituto CNR di Biotecnologie Applicate alla Farmacologia* of Catanzaro (Italy) for the computational support.

## References and Notes

1. Whitehouse, P. J.; Price, D. L.; Struble, R. G.; Clark, A. W.; Coyle, J. T.; Delon, M. R. *Science* **1982**, *215*, 1237.
2. Cutler, N. R.; Sramek, J. J. *Prog. Neuropsychopharmacol. Biol. Psychiatry* **2001**, *25*, 27.
3. Galisteo, M.; Rissel, M.; Sergent, O.; Chevanne, M.; Cillard, J.; Guillouzo, A.; Lagadic-Gossmann, D. *J. Pharmacol. Exp. Ther.* **2000**, *294*, 160.
4. Carelli, V.; Liberatore, F.; Scipione, L.; Impicciatore, M.; Barocelli, E.; Cardellini, M.; Giorgioni, G. *J. Contr. Rel.* **1996**, *42*, 209.
5. AChE complexes or adducts reporting ligands within the catalytic gorge of the enzyme have been only considered.
6. The PDB model *2ACE* contains the ACh bonded to the active enzyme in a tetrahedral geometry to the oxygen atom of the Ser200, which is the amino acid responsible for the catalytic hydrolysis attack. In such reference models are included 554 amino acids and 209 water molecules without H atoms.
7. McDonald, D. Q.; Still, W. C. *Tetrahedron Lett.* **1992**, *33*, 7743.
8. MacroModel ver 6.0 Mohamadi, F.; Richards, N. G. J.; Guida, W. C.; Liskamp, R.; Lipton, M.; Caufield, C.; Chang, G.; Hendrickson, T.; Still, W. C. *J. Comput. Chem.* **1990**, *11*, 440.
9. Backbone RMS deviation in Å between the active site of 2ACE and seven AChE models as published in Protein Data Bank (in parenthesis the PDB codes): 0.30 (1ACJ), 0.31 (1ACL), 0.30 (1CFJ), 0.28 (1EVE), 0.32 (1OCE), 0.19 (1VOT), 0.17 (2ACK).
10. Still, W. C.; Tempczyk, A.; Hawley, R. C.; Hendrickson, T. *J. Am. Chem. Soc.* **1990**, *112*, 6127.
11. *GRID v. 17*; Molecular Discovery Ltd.: Oxford, 1997. Goodford, P. J. *J. Med. Chem.* **1985**, *28*, 849.
12. Tacking into account the nature of the chemical moieties of ACh and **1** the following GRID probes have been considered: C3 for the methyl and methylene groups, OSP2 for the carbonyl oxygen, OES one for the ester oxygen and NM3 for the trimethylammonium moiety. The resolution of the calculations has been fixed to 3 points/Å.
13. *Spartan ver. 5.0*; Wavefunction, Inc.: Irvine, CA, 1997.
14. Inoue, A.; Kawai, T.; Wakita, M.; Iimura, Y.; Sugimoto, H.; Kawakami, Y. *J. Med. Chem.* **1996**, *39*, 4460.
15. (a) Donepezil, Decamethonium and Galantamine are known AChE inhibitors with most of the C atom positions well predicted by the C3 probe. Kryger, G.; Silman, I.; Sussman, J. L. *Structure Fold Des.* **1999**, *7*, 297. (b) Sussman, J.; Harel, M.; Frolow, F.; Oefner, C.; Goldman, A.; Toker, L.; Silman, I. *Science* **1991**, *253*, 872. (c) Greenblatt, H. M.; Kryger, G.; Lewis, G.; Silman, I.; Sussman, J. L. *FEBS Lett.* **1999**, *463*, 321.
16. Acetylcholinesterase (AChE) type XII-s from bovine erythrocytes (0.35 Units/mg solid) was purchased from Sigma-Aldrich.
17. Ellman, G. L.; Courtney, K. D.; Andres, V.; Featherstone, R. M. *Biochem. Pharmacol.* **1961**, *7*, 88.
18. Acetylcholinesterase activity were assayed with a double beam UV–Vis Lambda 40 Perkin–Elmer spectrophotometer, using 1 cm quartz cell containing 3 mL of 0.01 M (pH 7.4) phosphate buffer, 0.25 mM of DTNB and 10–250 mM of Atch, kept at 25 °C. In these conditions no autohydrolysis of Atch was observed. The above solutions were added to AChE (final concentration was 0.083 U/mL) and the changes in the absorbance at 412 nm were recorded between 0.5 and 1.5 min after enzyme addition.
19. Thanei-Wyss, P.; Waser, P. *Eur. J. Pharmacol.* **1989**, *172*, 165.
20. $^1$H NMR spectra were recorded on a Bruker AMX-500 spectrometer (11.4 Tesla).

## Supplementary Material

**Table 4.** List of the 109 residues selected in the 2ACE model within 10 Å form the SER 200

| Fragment | Amino acid list |
|---|---|
| 1 | ASN66 |
| 2 | GLN69 |
| 3 | TYR70-VAL71-ASP72-GLU73-GLN74-PHE75-PHE78-SER79-GLY80-SER81-GLU82-MET83-TRP84-ASN85-PRO86-ASN87 |
| 4 | TRP114-ILE115-TYR116-GLY117-GLY118-GLY119-PHE120-TYR121-SER122-GLY123-SER124-SER125-THR126-LEU127-ASP128-VAL129-TYR130 |
| 5 | LEU146-SER147-TYR148-VAL150-GLY198-GLU199-SER200-ALA201-GLY202-GLY203-ALA204-SER205 |
| 6 | LEU224-GLN225-SER226-GLY227-SER228 |
| 7 | CYS231-PRO232-TRP233-ALA234 |
| 8 | ARG244 |
| 9 | ILE275-ASP276-VAL277-GLU278-TRP279-ASN280-VAL281-LEU282-PRO283-PHE284-ASP285-SER286-ILE287-PHE288-ARG289-PHE290-SER291 |
| 10 | VAL293 |
| 11 | GLY322-ASN324-ASP326-GLU327-GLY328-SER329-PHE330-PHE331-LEU332-LEU333-TYR334-GLY335-ALA336 |
| 12 | LYS341 |
| 13 | LEU358 |
| 14 | PRO361 |
| 15 | VAL395 |
| 16 | ASN399-VAL400 |
| 17 | LEU430-VAL431 |
| 18 | TRP432-PRO433 |
| 19 | MET436-GLY437-VAL438-ILE439-HIS440-GLY441-TYR442-GLU443-ILE444-GLU445 |
| 20 | PHE448 |

**Table 5.** Full list of the atomic charges computed with Macro Model AMBER*, AM1 Efit e 3-21 G* Efit

| Atom description | Macro Model AMBER* ACh | Macro Model AMBER* 1 | AM1 Electrofit ACh | AM1 Electrofit 1 | 3–21 G* Electrofit ACh | 3–21 G* Electrofit 1 |
|---|---|---|---|---|---|---|
| C 1 | 0.141 | 0.141 | −0.116 | −0.189 | −0.300 | −0.360 |
| C 2 | 0.141 | 0.141 | −0.213 | −0.225 | −0.346 | −0.319 |
| C 3 | 0.141 | 0.141 | −0.151 | −0.163 | −0.399 | −0.381 |
| N + | −0.024 | −0.024 | 0.264 | 0.316 | 0.245 | 0.254 |
| C 5 | 0.180 | 0.180 | −0.210 | −0.157 | −0.176 | −0.329 |
| C 6 | 0.174 | 0.174 | 0.231 | 0.170 | 0.274 | 0.436 |
| O 7 | −0.400 | −0.400 | −0.526 | −0.476 | −0.594 | −0.647 |
| Ester $sp^2$ carbon | 0.600 | 0.600 | 0.793 | 0.760 | 0.909 | 1.049 |
| O 9 | −0.450 | −0.450 | −0.526 | −0.585 | −0.665 | −0.632 |
| C 10 | −0.115 | 0.000 | −0.399 | −0.019 | 0.321 | −0.668 |

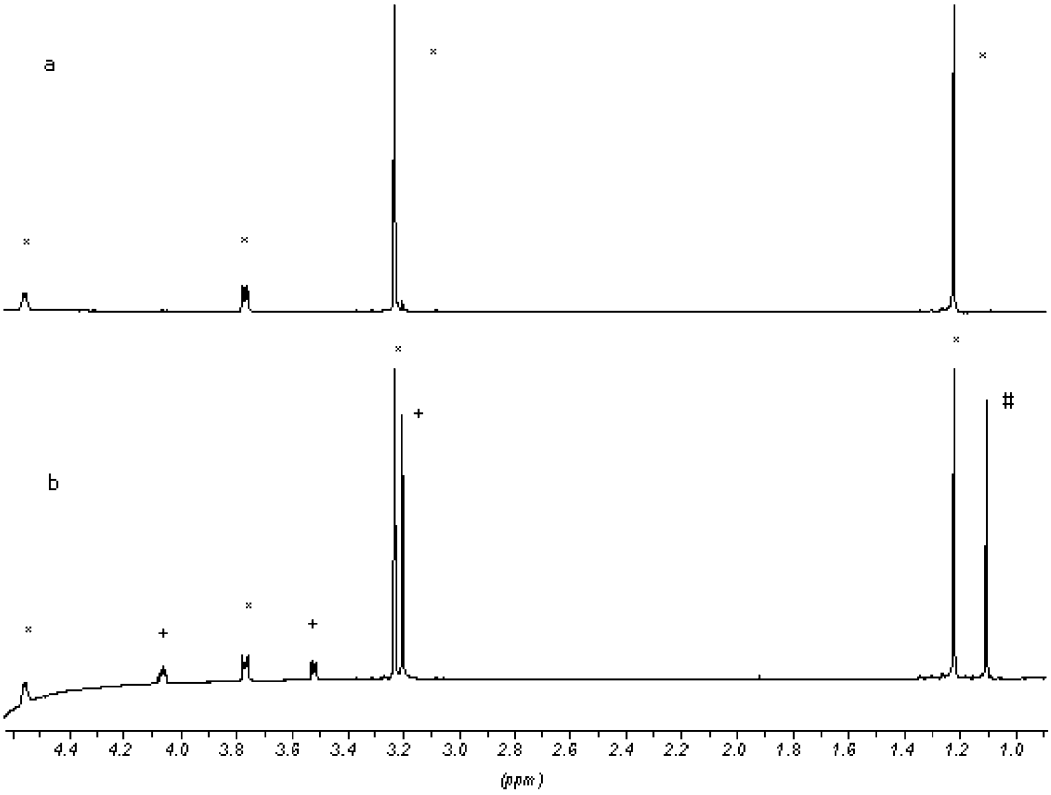


**Figure 5.** (a) $^{1}H$ NMR spectra of compound **1** (*). (b) After 24 h incubation with AChE, the choline protons are indicated as + and pivalate as #. Chemical shifts are given relative to the $D_2O$ signal at 4.78 ppm.